

## Florida Current: Seasonal and Interannual Variability

**Abstract.** Annual and interannual variations in the Florida Current, Caribbean, and subtropical Atlantic are investigated with the use of historical sea level differences and wind field data. Observational and model evidence suggests that the seasonal transport cycle of the Florida Current is locally forced, either upstream in the Caribbean or downstream over topography. Although at seasonal and shorter periods sea level or bottom pressure fluctuations on the left side of the Florida Current contribute almost all of the variance of sea level difference across the Florida Straits and hence transport, this relation does not seem to apply at interannual time scales. Using results from the Subtropical Atlantic Climate Studies, it is estimated from historical sea level data that interannual transport fluctuations of the Florida Current are only of order  $1 \times 10^6$  cubic meters per second. Interannual fluctuations in the 2- to 3-year period range in the Florida Straits seem to be correlated with sea level differences across the Caribbean and the subtropical Atlantic but not with Sverdrup transport fluctuations in the subtropical Atlantic.

Sea level measurements from both sides of the Florida Straits, from stations in the Caribbean, and from stations in the subtropical Atlantic (Fig. 1a) have been studied here in an attempt to estimate the magnitude of Florida Current transport variations at periods longer than those covered thus far in the Subtropical Atlantic Climate Studies (STACS) program by various other methods and described in the companion papers in this set (1-4) and also to obtain some insight into their possible relations to fluctuations in the Caribbean and in the subtropical North Atlantic east of the Bahamas. Recent model studies relevant for understanding these fluctuations are also reviewed.

A first determination of the mean Florida Current transport and its approximate range of seasonal variation was given by Niiler and Richardson (5) in an evaluation of 90 transport transects taken with the dropsonde technique but scattered over several years. The mean transport off Miami was found to be  $29.5 \times 10^6$  m<sup>3</sup>/sec, and the fit of a sinusoidal annual variation yielded a maximum of  $33.6 \times 10^6$  m<sup>3</sup>/sec in early summer and a minimum of  $25.4 \times 10^6$  m<sup>3</sup>/sec in early winter. However, monthly means of voltages measured during 1970 through 1972 over the cable running from Jupiter, Florida, to Settlement Point, Bahamas, and also of sea level differences across the Florida Straits measured over several years (6) indicated that the annual cycle must be quite asymmetric, with the most prominent feature the sharp drop from the seasonal maximum in July-August to the minimum in October-November. Figure 1b shows the annual cycles for sea level differences from Bimini to Miami during 1965 through 1972 and from Cat Cay to Miami for an earlier 5-year period. The voltage measurements of Sanford (6) for 1970 through 1972 are shown in Fig. 1c.

Monthly means of transports mea-

sured by moored current meters during STACS (1) are also included in Fig. 1c. All these annual cycles indicate a secondary maximum in March-April.

At periods of the fluctuations ranging from days to months the sea level or subsurface pressure measurements on the left side of the stream are very well correlated with transport, as shown by Maul *et al.* (4). At the annual period, which was not yet significantly resolved in STACS, sea levels on the left side of the Florida Channel when corrected for steric effects contain all the variation whereas the right side (Bimini) shows almost no response. Seasonal-corrected sea level curves from stations along the U.S. East Coast north of the Florida Channel still show the minimum in July and maximum in October but also an unexplained secondary minimum in February—as shown by Blaha (7). However, as also shown in (7), local wind setup, although negligible in the Florida Straits, is a major contributor to coastal sea level fluctuations north of the Channel and would play a role in this wintertime minimum.

The Gulf Stream has a downstream sea level slope, known as the Bernoulli head (8), which has a mean of 8.6 cm between Key West and Miami (9). The seasonal cycle of this sea level difference corresponds quite closely to that of the sea level difference across the Straits (correlation, 0.93) (Fig. 1b).

Sea level differences across the western Caribbean (line C in Fig. 1a) show an annual cycle similar to that of the Florida Current, with a maximum in summer and a minimum in fall. The correlation with the Bimini-Miami annual cycle is 0.83, and the range is almost the same (10). This is consistent with continuous throughflow between line C and the Florida Straits. Farther east, along line D in Fig. 1a, the maximum in July and minimum in October are still there, but a second minimum occurs in May and the

correlation with Bimini-Miami is lower.

How is the seasonal transport cycle of the Florida Current with its strong asymmetry (Fig. 1b) generated? On the basis of simplest Sverdrup dynamics (11), the wind stress curl between the Bahamas and Africa should generate an annually reversing Sverdrup transport of approximately  $\pm 15 \times 10^6$  m<sup>3</sup>/sec across 30°N between the Bahamas and Africa (Fig. 1d), which in turn should cause an annually reversing western boundary current of that magnitude flowing northward in December through April and southward in May through November. Farther south, across 20°N, the seasonal amplitude is only  $\pm 7 \times 10^6$  m<sup>3</sup>/sec but it has the same phase as the transport across 30°N (Fig. 1d). Obviously, these simple dynamics cannot explain the Florida Current transport cycle (Fig. 1b), which has an amplitude of only about  $\pm 3 \times 10^6$  m<sup>3</sup>/sec and is almost out of phase with what could be expected for the western boundary current caused by Sverdrup type annual wind forcing.

Recently, numerical model studies relevant for the annual wind forcing of the North Atlantic have been carried out. Anderson and Corry (12), using a two-layer model with 1° by 1° resolution, realistic bottom topography, and realistic boundaries including the Bahamas-Antilles island arc and some passages in between, driven by seasonally varying winds, were able to reproduce a Florida Current with an annual cycle very similar to that observed although of smaller amplitude. In that model simulation a large (about  $\pm 15 \times 10^6$  m<sup>3</sup>/sec) annually reversing barotropic current resulted east of the Bahamas, flowing northward in winter and southward in summer-fall, in agreement with the above Sverdrup argument. In a model run with constant water depth throughout the model domain (12), this large annual signal penetrated through the island passages and the Florida Straits and the Florida Current annual cycle looked very much like curve 3 in Fig. 1d with a range of  $\pm 15 \times 10^6$  m<sup>3</sup>/sec. The conclusion there is that the response at the annual period is dominantly barotropic and therefore cannot penetrate across topography through the Caribbean into the Florida Straits. Another seasonal model study with a multilayer model was recently carried out by Sarmiento (13), using wind forcing and 2° by 2° resolution with a smoothed bottom topography, that is, not resolving passages and the Florida Straits. He obtained a transport cycle for the region over the topography off Florida similar to the observed cycle but also smaller than that in (12). But in this case,

the transport cycle east of the topography is much smaller than in (12), only about  $\pm 5 \times 10^6$  m<sup>3</sup>/sec, but again with the phase of the Sverdrup forcing, northward in winter and southward in summer-fall.

Observational evidence such as that derived from 1-year moored current measurements east of the Bahamas (14) does not support the existence of a reversing boundary current there. If such a reversing recirculation actually exists, it must be a rather unfocused stream with low speeds in midbasin instead of a boundary jet along the outer Bahamas. In summary, there is conflicting modeling and observational evidence on the effect of seasonal wind forcing over the subtropical Atlantic for the western boundary currents.

Another possibility for generating the seasonal Florida Current variation is local wind forcing upstream or downstream. We find the same type of seasonal asymmetry in the negative wind stress

curl calculated from the data set of Hellerman and Rosenstein (15) over the western Caribbean (Fig. 1d). A more detailed investigation of historical wind data by Elliott (16), in which monthly means of the curl field were determined on 4° squares and then averaged over the area of the Cayman Basin, showed an even closer relationship (correlation, 0.93) with the annual cycle of sea level difference across the Florida Straits. When integrated across the basin, this wind stress curl variation amounts to a seasonal cycle of  $\pm 5 \times 10^6$  m<sup>3</sup>/sec. In the numerical model study of Anderson and Corry (12) wind forcing when applied only to the area west of the island arc yielded an annual cycle very similar to that of the Florida Current variation, although of only small amplitude ( $\pm 0.5 \times 10^6$  m<sup>3</sup>/sec). However, here only a homogeneous ocean was considered. Another possibility would be forcing north of the Florida Straits over topography where the wind stress curl

and also the meridional wind stress component have annual cycles similar to that of the Florida Current. Florida Current modification then would be through a southward-propagating baroclinic Kelvin wave (17).

The above argument about the possible local forcing of the annual cycle and its decoupling from the open North Atlantic does not mean that the Florida Current could not be a good indicator of lower frequency transport changes in the open Atlantic. At the annual period the response in the Atlantic is dominantly barotropic; the island arc effectively shelters the Florida Straits from the interior barotropic boundary current. At sufficiently long time scales, baroclinic adjustment compensates for the effect of bottom topography, and the interior fluctuations can penetrate through the Caribbean and the Gulf of Mexico to the Florida Straits.

To investigate the magnitude of interannual variability of the Florida Current

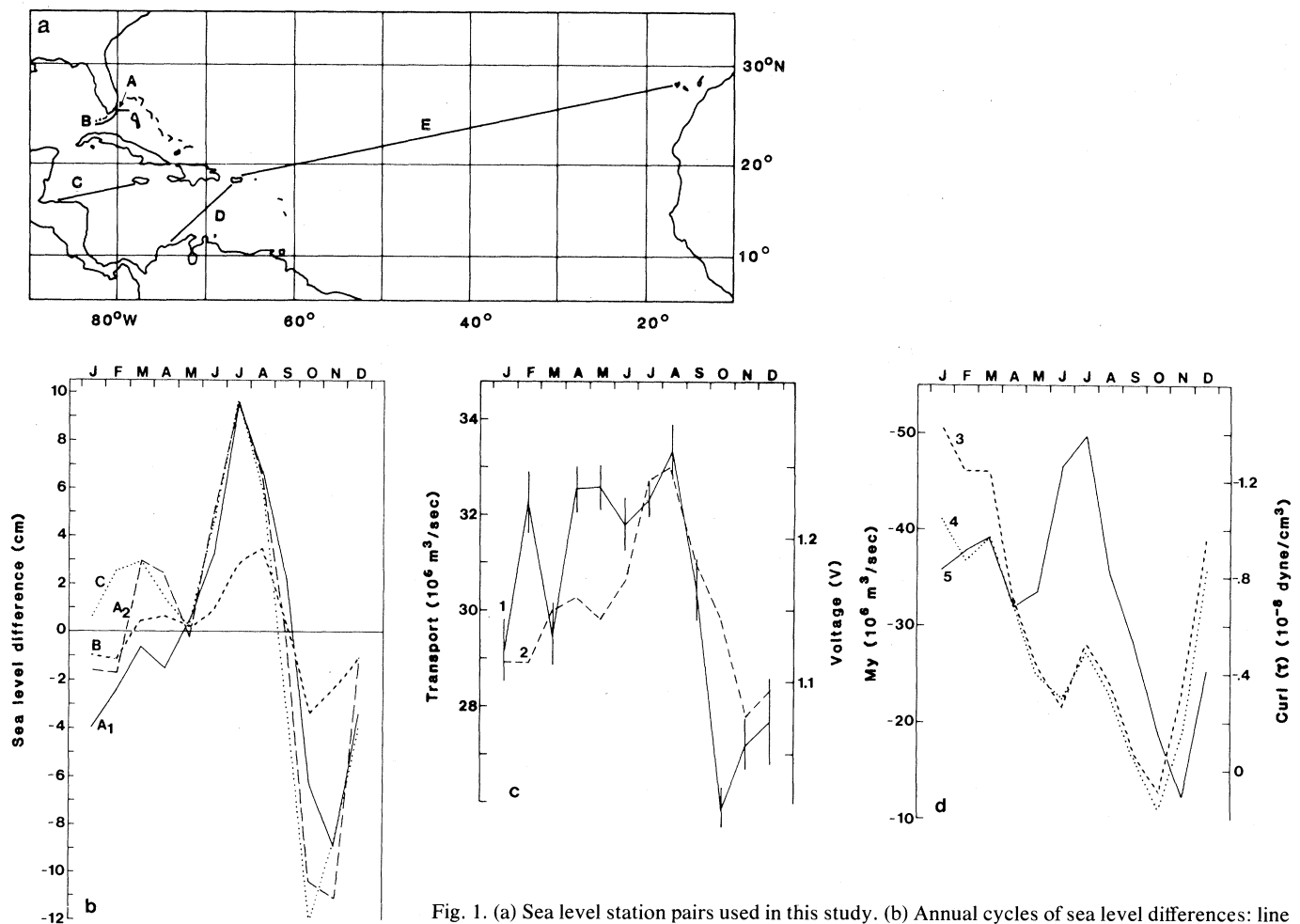


Fig. 1. (a) Sea level station pairs used in this study. (b) Annual cycles of sea level differences: line A<sub>1</sub>, Bimini to Miami (1965 to 1972); line A<sub>2</sub>, Cat Cay to Miami (1938 to 1941, 1950 to 1951); line B, Key West to Miami; line C, Jamaica to Honduras. (c) Annual cycles: curve 1, STACS transports from moored current meter measurements (with standard deviations of the monthly means); the gap in December to February [figure 1 in (1)] was filled in with STACS cable transports (3); curve 2, cable voltages for 1970 through 1972 [from (6)]. (d) Annual cycles: curve 3, Sverdrup transport  $M_y$  (mass transport, north-south component) across 30°N [from (15)]; curve 4, same as curve 3 except that wind stress from (22) is used; curve 5, wind stress curl over the Caribbean [from (15)]; the offset between both scales is arbitrary.

and its possible relation to changes in the Caribbean and subtropical Atlantic we present (in Fig. 2a) interannual variations of sea level differences across the subtropical Atlantic (sea level at San Juan, Puerto Rico, minus sea level at Tenerife, Canary Islands); across the eastern Caribbean (Magueyes Island minus an average of two stations in Colombia, Riohacha and Cartagena); across the western Caribbean (Port Royal, Jamaica, minus an average of two stations in Honduras, Puerto Cortes and Puerto Castilla); and Bimini minus Miami. The time series are low-passed with a Lanczos filter with 18-month half-power period.

The similarity of the annual cycles of the Florida Current Bernoulli head with the cross-stream slope and transport (Fig. 1b) suggested that the sea level differences between Key West and Miami might be a useful Florida Current transport indicator; STACS results for shorter time periods even showed that the Miami record alone was very well correlated with transports (4). This would yield transport time series since about 1920 when these tide gauge stations were established. Unfortunately, at longer than annual periods, the sea level difference is determined mostly by fluctuations on the Bimini side, and sea level

Miami or Key West–Miami differences are not significantly correlated with the Bimini–Miami differences.

Even from the few years of Bimini–Miami sea level differences, we can get a rough estimate of the interannual transport variability of the Florida Current. From the annual cycle (Fig. 1, b and c) we know that a change in sea level difference of 1 cm between Bimini and Miami corresponds to a transport change of about  $0.4 \times 10^6 \text{ m}^3/\text{sec}$ . The low-passed interannual variability curve for the sea level difference (Fig. 2a) shows root-mean-square amplitudes of 3.6 cm. Applying the above relation between transport and sea level slope would yield an interannual transport variability of order  $\pm 1.4 \times 10^6 \text{ m}^3/\text{sec}$ . It may even be smaller if the transport profile in the Straits is more baroclinic at interannual periods than at seasonal and shorter periods for which the relation between sea level difference and transport was derived and for which transport fluctuations are dominantly barotropic (18).

Sea level differences across the subtropical Atlantic and the Caribbean show periods and amplitudes similar to those across the Florida Current. The records for Tenerife and San Juan have been corrected for air-pressure anomaly, but

the correction changes that time series of sea level differences only slightly. The two time series from the Caribbean have not been corrected.

It has to be considered whether thermal effects could be responsible for much of this interannual variability. There are not enough stratification data available for a satisfactory evaluation at the different stations, but one can make a rough estimate of the surface mixed-layer effects by using sea-surface temperature (SST) values from the Marine Deck (19). In the Caribbean and near the other stations used (Fig. 1a) interannual SST variations, treated in the same way as the sea level differences in Fig. 2a, had maximum amplitudes of  $0.5^\circ\text{C}$ .

If we assume this anomaly to be constant throughout the depth of the mixed layer, about 100 m (20), the corresponding sea level anomaly is 1.5 cm, not negligible but significantly less than the observed sea level variations. Its effect across the Caribbean is reduced even further by the fact that the observed SST variations were very similar and in phase in the area of lines C and D (Fig. 1a). SST anomalies from near the Canary Islands and near Puerto Rico were not correlated with the sea levels at Tenerife and San Juan, respectively, indicating a minor effect of near-surface heat storage anomalies on the sea level difference along line E on the time scales of a few years that dominate these records.

The fluctuations at lines D and E (Fig. 2a) are about equal in amplitude and in phase, which seems to suggest that southward geostrophic transport across line E corresponds to northward return flow through the Caribbean across line D. In turn, sea level differences along lines C and D seem correlated with Florida Current sea level differences. Time lags between the time series from the different lines are not significant.

If we assume that all the transport anomalies across lines E and C would flow through the Florida Straits, this would give an estimate of these anomalies of only  $\pm 1 \times 10^6 \text{ m}^3/\text{sec}$ . To estimate geostrophic transports across line E directly, we need to assume a vertical transport profile. There are two limiting cases. One is a barotropic velocity profile, resulting in a transport of  $6 \times 10^6 \text{ m}^3/\text{sec}$  per 1-cm sea level difference. The other alternative is to assume that for these interannual variations across lines C, D, and E the geostrophic transport profile decreases quickly with depth. If it is approximated by a linear decrease from the surface down to 800 m as done for the mean wind-driven transport across  $24^\circ\text{N}$  by Leetmaa *et al.* (21), the

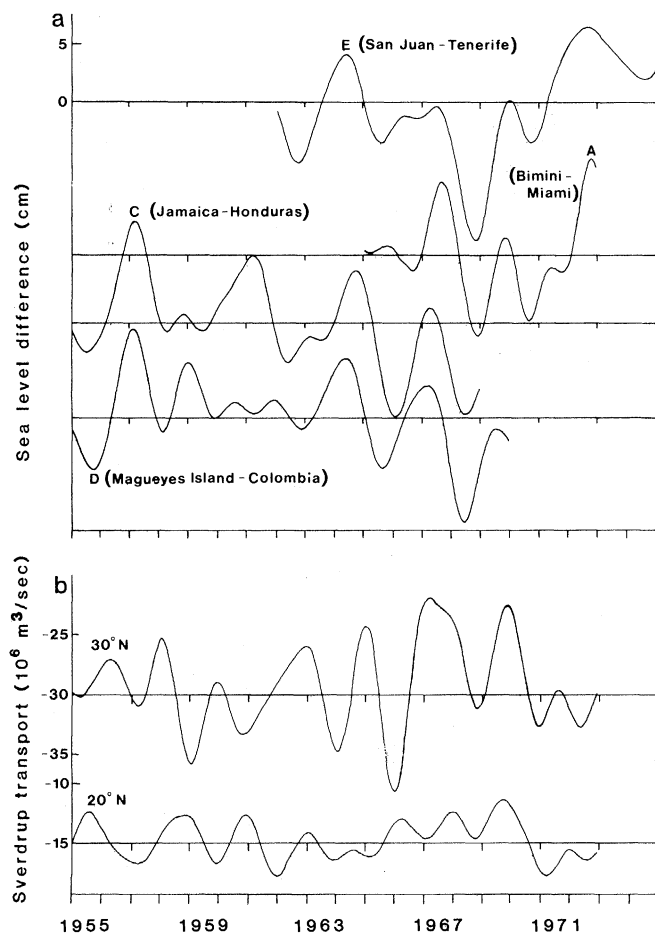


Fig. 2. (a) Interannual variability of sea level differences (18-month low-passed) across the Florida Straits (line A), the Caribbean (lines C and D), and the interior North Atlantic (line E). (b) Interannual variability of Sverdrup transport (18-month low-passed) across  $20^\circ\text{N}$  and  $30^\circ\text{N}$ , determined from (22).

geostrophic transport anomaly is only  $0.6 \times 10^6 \text{ m}^3/\text{sec}$  per 1-cm sea level difference. For the root-mean-square amplitude of 4.2 cm of the sea level difference along line E the latter assumption would result in a root-mean-square transport fluctuation of  $2.5 \times 10^6 \text{ m}^3/\text{sec}$ , still larger by a factor of 2 than our Florida Current transport estimate, whereas for a barotropic velocity assumption this value would be about ten times as much.

One has to bear in mind here that this transport fluctuation can only show the net geostrophic flow between Tenerife and San Juan, not any recirculation of southward flow in midbasin within line E east of Puerto Rico.

Time series anomalies of Sverdrup transport between Africa and the western boundary, again low-passed with an 18-month cutoff period, are given in Fig. 2b for  $30^\circ\text{N}$  and  $20^\circ\text{N}$ . They are calculated from the monthly means of wind stresses of Bunker and Goldsmith (22) for a  $10^\circ$  by  $10^\circ$  grid. Despite this rather coarse resolution, the integrated wind stress curl fields agree reasonably well with the finer resolution curls from Helleman and Rosenstein (15), at least at the annual period (Fig. 1d). Hence, the time series for transports across  $20^\circ\text{N}$  and  $30^\circ\text{N}$  as shown in Fig. 2b should give an idea of the magnitude of interannual variations. Root-mean-square amplitudes are  $4.8 \times 10^6 \text{ m}^3/\text{sec}$  at  $30^\circ\text{N}$  and  $2.1 \times 10^6 \text{ m}^3/\text{sec}$  at  $20^\circ\text{N}$ . This is the same order of magnitude as the geostrophic transport estimate across line E (Fig. 1a) that one would attain from sea level differences (Fig. 2a), assuming the baroclinic profile, but correlation between the Sverdrup transports (or their geostrophic component after elimination of the Ekman transport) and sea level differences is not significant. Even if wind forcing were the only factor causing this variability with periods of a few years, the lack of correlation would not be unexpected. Although at the annual period the response is mostly barotropic and therefore generates a western boundary current immediately, Anderson and Corry (17) have estimated that it would take about a decade to establish Sverdrup equilibrium in a basin of the scale of the subtropical North Atlantic because of the slow propagation speed of the baroclinic Rossby wave. This conclusion is also supported by a recent numerical model calculation with a six-layer model,  $2^\circ$  resolution, driven by the winds of Bunker and Goldsmith (22) in which Willebrand and Olbers (23) obtained a small interannual variation of the western boundary current transport

that was not correlated with the Sverdrup transport of Fig. 2b. In an earlier study with a barotropic model and winds of Bunker and Goldsmith (22), Willebrand *et al.* (24) showed for a time segment of several years that the resulting western boundary current transport closely resembled the Sverdrup transport across  $40^\circ\text{N}$ .

Another mechanism to be considered is thermohaline forcing, which drives a meridional circulation cell at  $24^\circ\text{N}$  of about  $15 \times 10^6 \text{ m}^3/\text{sec}$  of warm water going north above 1000 m and returning at depth (25). The variability of this vertical gyre on the interannual time scale is not known, except that transports and heat flux in 1957 (the International Geophysical Year) and 1981 as determined by inverse methods (25) were very similar; this similarity could have been a coincidence. Modeling with interannual thermohaline-forcing anomalies is needed, but the data base is much sparser and more doubtful than for the wind fields.

FRIEDRICH SCHOTT  
RAINER ZANTOPP

*Rosenstiel School of Marine  
and Atmospheric Science,  
University of Miami,  
Miami, Florida 33149*

#### References and Notes

1. T. Lee, F. Schott, R. Zantopp, *Science* **227**, 298 (1985).
2. R. L. Molinari, W. D. Wilson, K. Leaman, *ibid.*, p. 295.
3. J. C. Larsen and T. B. Sanford, *ibid.*, p. 302.

4. G. A. Maul, F. Chew, M. Bushnell, D. A. Mayer, *ibid.*, p. 304.
5. P. Niiler and W. S. Richardson, *J. Mar. Res.* **31**, 144 (1973).
6. T. Sanford, *ibid.* **40** (Suppl.), 621 (1982). Sea level differences in that study were between means from Cat Cay (Bahamas) and Miami, taken, for different time periods, from J. Patullo *et al.* [*ibid.* **14**, 88 (1955)].
7. J. P. Blaha, *J. Geophys. Res.* **89**, 8033 (1984).
8. J. G. Charney, *Proc. Natl. Acad. Sci. U.S.A.* **41**, 731 (1955).
9. F. Chew, E. Balazs, C. Thurlow, *Oceanol. Acta* **5**, 21 (1982).
10. These sea levels are corrected by atmospheric pressure for the inverse barometric effect. Florida Current stations were not corrected because of their proximity.
11. In Sverdrup balance, the meridional transport per unit width is equal to the wind stress curl divided by beta, the meridional derivative of the Coriolis parameter.
12. D. A. Anderson and R. A. Corry, in preparation. In this case not the winds from (15) but those from (22) at  $1^\circ$  resolution were used.
13. J. Sarmiento, personal communication; he used the winds of (15).
14. D. Olson, F. Schott, R. Zantopp, K. Leaman, *J. Phys. Oceanogr.*, in press.
15. S. Helleman and M. Rosenstein, *ibid.* **13**, 1093 (1983).
16. B. Elliott, *Eos* **64**, 236 (1983).
17. D. Anderson and J. Corry, *Prog. Oceanogr.*, in press.
18. In fact, cable voltages for 1969 to 1974 converted into transports by J. C. Larsen (personal communication) with the STACS results from (3) showed an amplitude of 18-month low-passed interannual variation of less than  $1 \times 10^6 \text{ m}^3/\text{sec}$ .
19. The Marine Deck is the compilation of historical marine observations between 1861 and 1960 in specified areas of the world oceans.
20. P. Lamb, *Tellus* **36**, 292 (1984).
21. A. Leetmaa, P. P. Niiler, H. Stommel, *J. Mar. Res.* **36**, 311 (1978).
22. A. Bunker and R. Goldsmith, *Woods Hole Oceanogr. Inst. Tech. Rep.* 79(3) (1979).
23. J. Willebrand and D. Olbers, personal communication.
24. J. Willebrand, S. G. H. Philander, R. C. Pacanowski, *J. Phys. Oceanogr.* **10**, 411 (1980).
25. D. Roemmich and C. Wunsch, in preparation.
26. This study was supported by the National Oceanic and Atmospheric Administration and the Office of Naval Research under contract N-00014-80-C-0042.

8 May 1984; accepted 19 November 1984

## Partial Primary Structure of the Alpha and Beta Chains of Human Tumor T-Cell Receptors

**Abstract.** *The T-cell receptor for antigen (Ti) was purified from the human tumor cell line HPB-ALL. Amino-terminal sequence analysis of an acid-cleaved peptide of the T $\alpha$  chain showed that it is highly homologous to a putative murine  $\alpha$  chain recently described. Amino-terminal sequence analysis of the T $\beta$  chain revealed that it shares 50 percent homology with the T $\beta$  chain amino acid sequences from two other human T-cell tumors. Nucleotide sequence analysis of a complementary DNA clone encoding the T $\beta$  chain from the HPB-MLT cell line showed that this chain represents a second human constant region gene segment and suggested that it arises from direct joining of the variable and joining gene segments without any intervening D region sequences.*

The T-cell receptor for antigen (Ti) has been serologically and biochemically identified as a 90-kilodalton (kD) heterodimer composed of disulfide-linked acidic ( $\alpha$ ) and basic ( $\beta$ ) glycoprotein chains of approximately 40 to 50 kD (1-3). Using differential hybridization techniques, two groups of investigators have identified a T-cell specific complementary DNA (cDNA) clone with a deduced amino acid sequence that is homologous to

the amino-terminal sequence of the  $\beta$  chain of Ti (4-6). This gene, which shows significant homology to immunoglobulin genes, is composed of variable (V), diversity (D), joining (J), and constant (C) region segments that undergo specific rearrangements during T-cell ontogeny (4-5, 7-11). Analysis of the murine genomic T $\beta$  gene, has revealed the existence of two constant region gene segments ( $C_{\beta 1}$  and  $C_{\beta 2}$ ) which are more